Urban Land-use Classification Using Variogram-based Analysis with an Aerial Photograph

Shuo-sheng Wu, Bing Xu, and Le Wang

Abstract

In this study, a variogram-based texture analysis was tested for classifying detailed urban land-use classes, such as mobile home, single-family house, multi-family house, industrial, and commercial from a digital color infrared aerial photograph. Spectral classification was first carried out to separate the building class from non-building classes. Then, a building-presence binary image was generated so that building pixels were assigned a value of "1" and non-building pixels were assigned a value of "0." Multiple texture bands were further generated employing a variogram-based texture analysis and used for land-use classification. The generation of the building presence binary image allowed us not only to fully explore the capability of variogram-based analysis on spatial pattern detection, but also to prevent the variogram-based analysis from being disturbed by the natural fluctuation of spectral signals. The result from using a mosaic test image was considered satisfactory with a kappa coefficient of 0.72.

Introduction

The urban environment contains a variety of spectrally different materials, such as soil, grass, trees, plastic, metal, shingle wood, and concrete. Traditional pixel-based spectral classifications assign each pixel to one of the candidate classes based on its brightness value, which indicates the spectral reflectance of the earth surface. However, using spectral information alone is not sufficient for classification of spectrally heterogeneous land-use classes, such as mobile home, single-family house, multi-family house, industrial, and commercial. Therefore, texture information from spatial patterns is often used to complement spectral information. New texture bands, in addition to original spectral bands, may be used together in classification. Each pixel in each of the texture bands is assigned a digital value as a reflection of the spatial variation of pixel brightness in the neighborhood in a sense of describing local textures.

There are several approaches of creating texture bands. The variogram of geostatistics, applied in a window-based function, is a relatively recent technique (Miranda *et al.*, 1992; Miranda and Carr, 1994). The variogram is commonly represented by a graph of semi-variance against the lag. The lag is the distance between paired data points. The semi-variance is half the average of the squared difference between paired data values. The mathematical function of the semi-variance (γ) by certain lag (h) can be expressed as (Burrough and McDonnell, 1998):

$$\gamma(\mathrm{h}) = \frac{1}{2n}\sum_{i=1}^{n}\left[z(\mathrm{x}_i) - z(\mathrm{x}_i + \mathrm{h})\right]^2$$

where n is the number of paired pixels; $z(\mathrm{x}_i)$ and $z(\mathrm{x}_i + \mathrm{h})$ are pixel values at x_i and $\mathrm{x}_i + \mathrm{h}$, respectively.

Variograms allow remote sensing researchers to measure the degree of spatial autocorrelation inherent in different landscapes as recorded in remote sensing images. However, the spectral values calculated in the variogram may be influenced by multiple factors, such as soil type, solar radiation, precipitation run off, flooding frequency, and wind direction. Each factor may have its own sub-variogram representing a unique autocorrelation structure, while a combined effect will create a summed, observed variogram. Burrough and McDonnell (1998) thus suggested that a pragmatic approach was to use a domain-specific variogram whenever possible. For this reason, we generated a building-presence variogram to describe spatial patterns alone. Rather than computing variograms directly using pixel gray values, we computed the variogram based on a binary image of buildings. The binary image will replace the original spectral image to serve as a base to extract autocorrelation information contributed by the building pattern alone. The rationale of using this binary image was not only to remove the effect of spectral fluctuation caused by a number of factors, but also to highlight and reserve the spatial patterns of buildings.

There have been two main approaches of using the variogram as texture measures in the field of remote sensing. One approach was that the variogram was modeled by a mathematical function and the coefficients of the function were used as texture measures. Some example studies included Ramstein and Raffy (1989), Herzfeld and Higginson (1996), Chen and Stow (2002), and Chen and Gong (2004). The other approach was to use semi-variance values at various lags as texture measures. Some example studies

Shuo-sheng Wu and Le Wang are with the Department of Geography, Texas State University-San Marcos, 601 University Drive, San Marcos, TX 78666-4616 (sw1020@txstate.edu; lewang@txstate.edu).

Bing Xu is with the Department of Geography, University of Utah, 260 S. Central Campus Dr., Rm. 270, Salt Lake City, UT 84112-9155 and also with the Department of Environmental Science and Engineering, Tsinghua University, Beijing, 100084, China (bing.xu@geog.utah.edu).

Photogrammetric Engineering & Remote Sensing
Vol. 72, No. 7, July 2006, pp. 813–822.

0099-1112/06/7207–0813/$3.00/0

included Carr (1996), Lark (1996), Berberoglu *et al.* (2000), Chica-Olmo and Abarca-Hernández (2000), and Maillard (2003).

When researchers used modeled variogram coefficients as texture measures, they assumed that the fitted model of a variogram best represented spatial characteristics of the studied object or phenomena. On the other hand, when researchers used individual semi-variance values as texture measures, they assumed that the semi-variance at certain lags best represented the spatial characteristics. The weakness of the first approach is that the modeled coefficients may not have sufficient discriminatory power for identifying different land-uses. On the other hand, although individual semi-variance values may contain more information, they require intensive computation and are sensitive to natural fluctuation of spectral signals. To overcome the problem due to spectral signal fluctuation, we computed the variogram based on the binary image of buildings. The use of a building-presence variogram instead of a pixel-gray-value variogram was expected to mitigate the problem of noisy signals.

Classifying urban land-uses has been a challenge for remote sensing researchers (Donnay *et al.* 2001). The objective of this study was to test variogram-based texture analysis for urban land-use classification. Specifically, we tested whether or not a building-presence variogram could effectively classify urban land-use. We first classified the building class using a common spectral classification approach. A building-presence image was then created by assigning building pixels a value of "1" and non-building pixels a value of "0." We then derived multiple semi-variance texture bands from the building-presence image; each pixel in the texture band was assigned a digital value of the semi-variance calculated at a certain lag in a surrounding neighborhood. A supervised classification procedure was finally operated based on multiple texture bands to get a final urban land-use map.

Study Area and Data Preparation

The study area is the City of Austin, the capital of Texas. Austin is a fast-growing city and has a variety of urban land-uses (COA, 2001). For the purpose of testing new approaches for urban land-use classification, we used a mosaic test image with eight types of urban land-use (Figure 1). Training images were also selected for each type of land-use separate from the mosaic test image (Figure 2). The images are two-foot (approximately 0.61 meters) spatial resolution, three band (green, red, near-infrared) color infrared digital orthophotos. We obtained the digital orthophotos from the City of Austin Planning Department. The original aerial photographs were taken in the year of 2000 by Analytical Surveys Incorporation contracted by the City. The land-use areas were arbitrarily selected throughout the Austin area. The major land-use types of the City's existing land-use inventory included mobile home, single family, multi-family, industrial, and commercial. Mobile home refers to trailers; single-family land-use refers to single houses; multi-family land-use refers to apartments or condominiums. We selected two specific types from each of the three major types of land-uses due to their significant difference of building patterns. The particular type of industrial land selected was a storage warehouse, and the commercial land selected was a shopping center. Existing land-use inventory of digital vector data from the City of Austin Planning Department were used as ground truth for evaluating classification results.

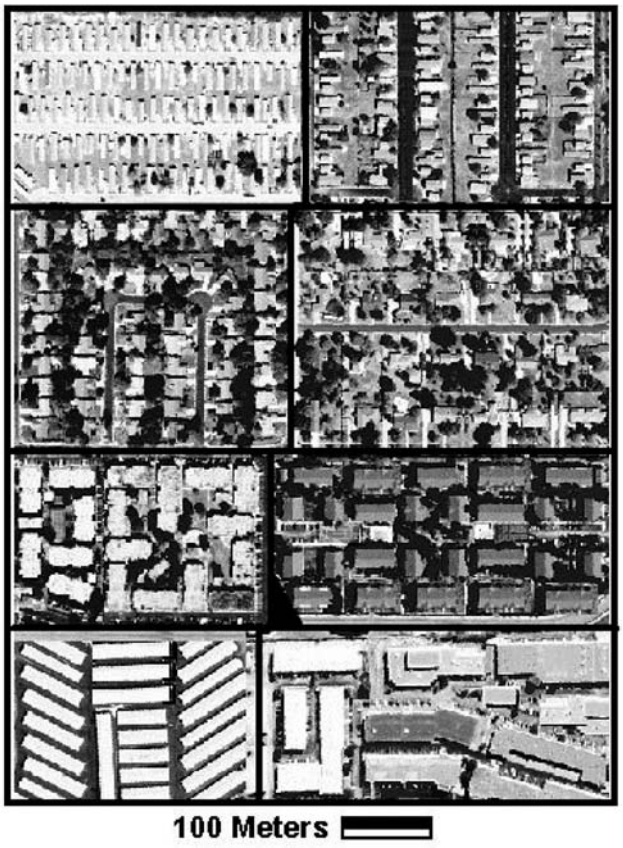

Figure 1. A mosaic test image of eight types of urban land-use, including, from left to right, top to bottom, mobile home I, mobile home II, single family I, single family II, multi-family I, multi-family II, industrial, and commercial. Mosaic boundaries are marked with black lines to distinguish between different types of land-use. The entire image size is 929 by 1,222 pixels.

Analysis

Classifying the Building Class

The first step of our variogram-based texture analysis was to classify the building class from the training and test image. We directly applied a K-Means unsupervised classification to automatically generate sixteen clusters and picked out clusters most representing the building class (Figure 3a). We then applied a 3 by 3 low pass filter twice to suppress speckles for deriving a better representation of the building class (Figure 3b). The same procedures were applied to the training images (Figure 4).

Observing Variogram Patterns

Before deriving semi-variance texture bands for classification, we calculated the average variogram from individual training images to observe how variogram relates to land-use (Figure 5a). The graph showed that all land-use variograms were different. Generally each land-use variogram reached a sill at a certain range. Mobile home I had the shortest range between 8 and 16 lags (approximately 2.4 and 4.9 meters, respectively), which may correspond to the relatively small structure size and short distances among the mobile homes. The sills of commercial, industrial, and multi-family I were higher than that of mobile home, single family, and multi-family II, which may be

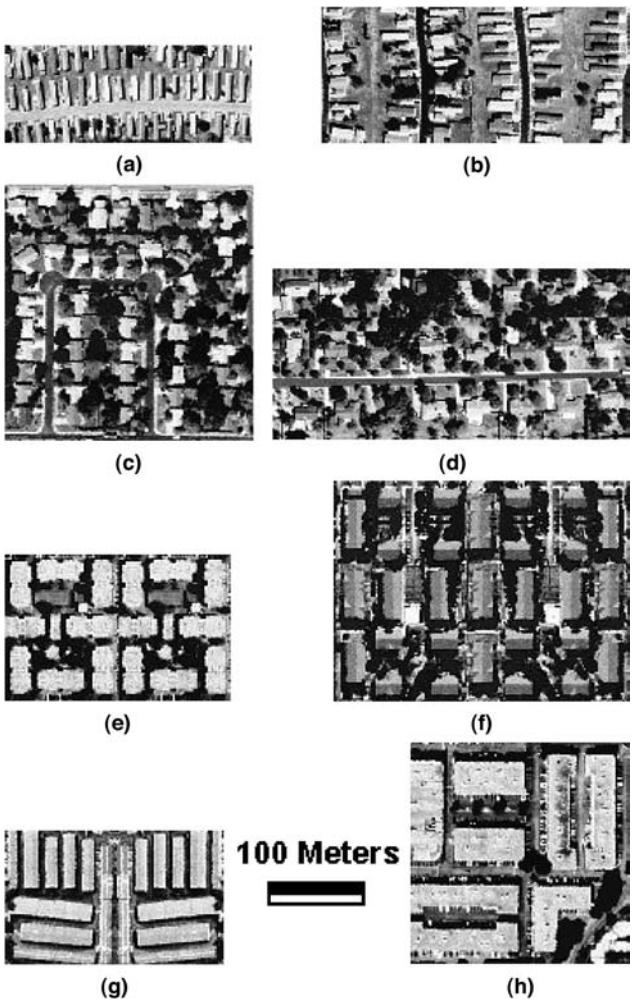

Figure 2. Training images for eight types of urban land-use, including, (a) mobile home I, (b) mobile home II, (c) single family I, (d) single family II, (e) multi-family I, (f) multi-family II, (g) industrial, and (h) commercial. The entire image size is 1,015 by 1,222 pixels.

interpreted that the former group of land-use had more heterogeneous spatial-autocorrelation structures of buildings than that of the later group.

Resampling Effects

To investigate resampling effects on variogram patterns, we resampled the original 2-foot resolution training images to 16-feet-resolution images and calculated their variograms (Figure 5b). Comparing Figure 5a and 5b, the general shape of all variograms were almost the same, although the resampled variograms were not as smooth and continuous as the originals. Since resampling procedure did not change much of the variogram patterns, we decided to use the resampled images so that we can efficiently test different approaches. The original 2-foot resolution mosaic test image was then resampled to a 16-foot resolution image (Figure 6).

Optimal Window Sizes and Lags

The semi-variance texture bands were created based on certain lags and certain pixel window sizes. Different window sizes were tested within the limit of the training image, and different lag sizes were tested within the limit of the window

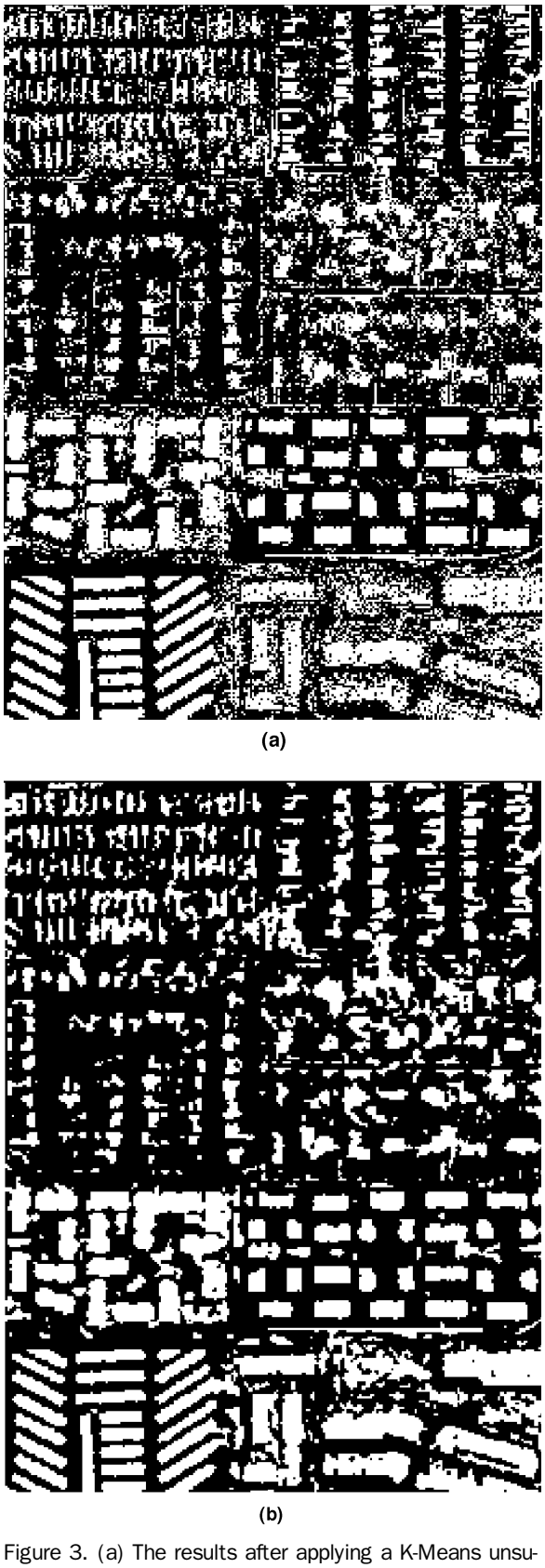

Figure 3. (a) The results after applying a K-Means unsupervised classification to the mosaic test image. White areas are mostly buildings and a few pavements of roads and drive ways. Black areas are other spectrally different materials. (b) The results after further applying low pass filters.

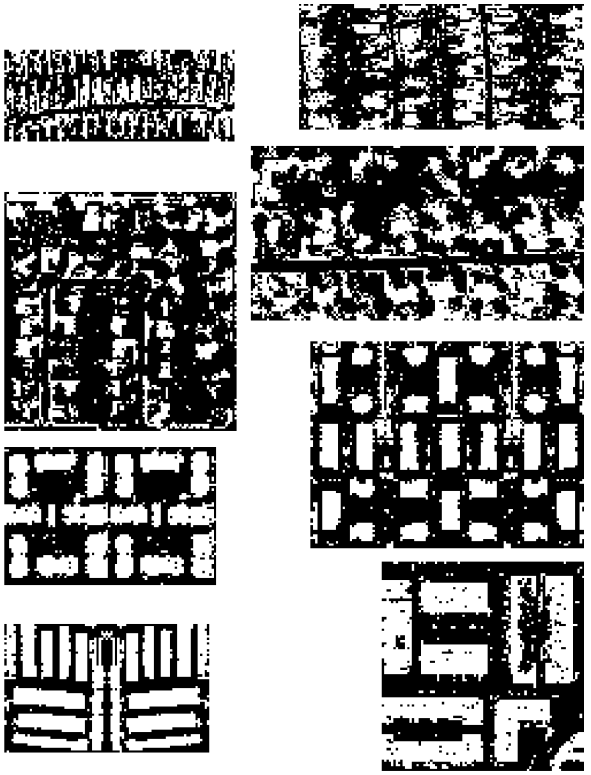

(a)

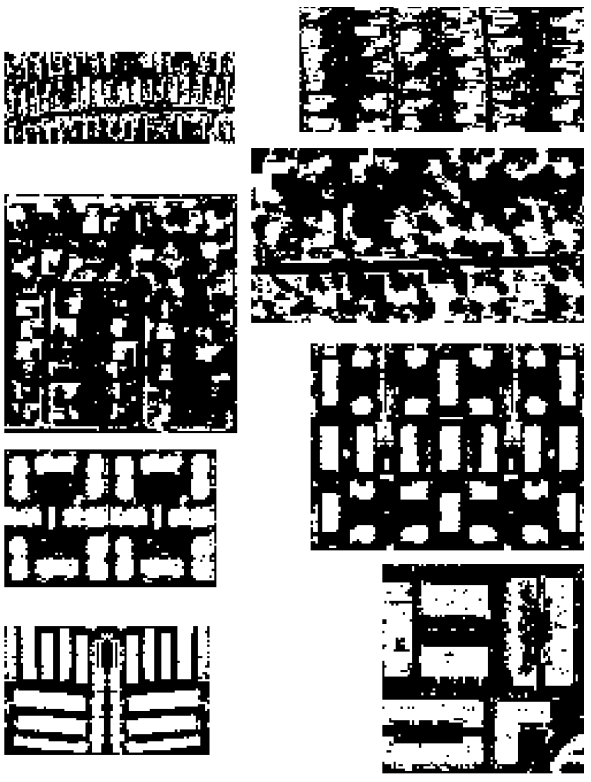

(b)

Figure 4. (a) The results after applying a K-Means unsupervised classification to training images. (b) The results after further applying low pass filters.

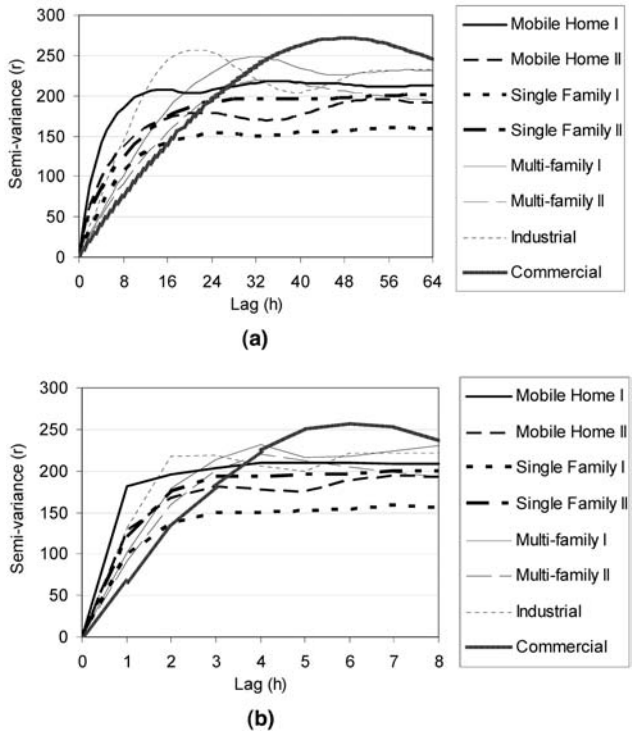

Figure 5. (a) The average variogram calculated from training images. Each lag distance was one pixel length (2 feet) and the semi-variance was rescaled 900 times. The scale factor was decided by experiment to allow the rescaled maximum close to a value of 255, which was the maximum pixel value allowed in an 8-bit image. (b) The average variogram calculated from resampled 16-feet-resolution training images. Each lag distance was one pixel length (16 feet) and the semi-variance was rescaled 900 times.

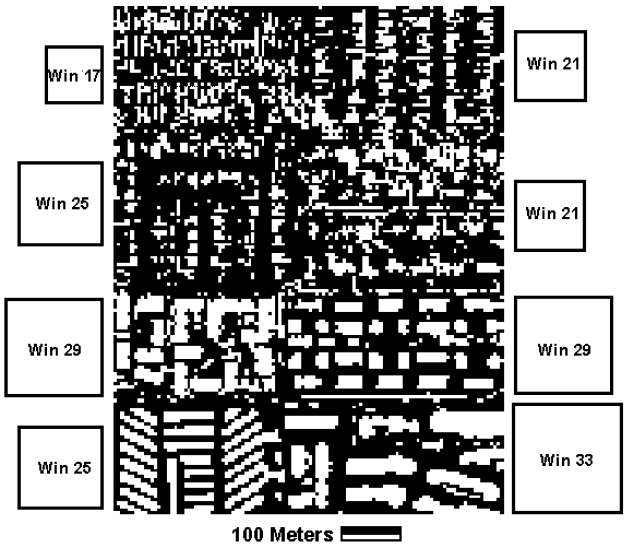

Figure 6. The 16-foot resolution mosaic test image resampled from the original 2-foot resolution image. The optimal window sizes for each land-use were drawn by the side in their actual scales.

size. The optimal window sizes and the optimal lags that could achieve the highest classification accuracy were investigated.

Optimal window sizes are selected based on better characterization of spatial patterns of land-use categories with less boundary effect. The boundary effect refers to the situation that assigning class for a pixel which is close to the boundary of two or more neighboring classes is confused within a window (Gong, 1994; Xu *et al.*, 2003). The dilemma was that the pixel window size should not be too small or too big. When the window was too small to contain enough building class pixels to analyze their spatial relationship, the derived semi-variance would not represent the texture well as a whole. When the window was too large, it straddled two neighboring classes and the derived semi-variance was a mixture of class textures. In other words, too small window sizes caused high within-class variation and too large windows caused high between-class confusion. Both extreme window sizes cast difficulty on the classification. This boundary effect was especially significant for our study area since it mainly comprised small parcels of urban land-use, in contrast to the commonly large, homogeneous parcels of rural land-use.

Optimal window sizes were usually decided empirically (e.g., Gong and Howarth, 1992; Xu *et al.*, 2003), so were optimal lags (e.g., Berberoglu *et al.*, 2000). Similarly, this study investigated the optimal window sizes and optimal lags through repeated experiments. Semi-variance texture bands in different window sizes and different lags were derived for both the mosaic test image and the training image. Training signatures for each land-use type were computed from training images based on certain combination of texture bands. Classifications using the Maximum Likelihood Classifier (MLC) were then operated based on different combinations of texture bands to investigate the optimal window sizes and optimal lags (Figures 7 through Figure 11).

We also investigated the optimal number of texture bands and the classifiers that achieved the best accuracy (Figure 12 and Figure 13). Accuracy assessment was based on 400 random samples with 50 for each class. In addition, we computed signature separability based on different combinations of texture bands to investigate whether or not training signature separability is a good predictor of classification accuracy.

Taking into account the size of land-use parcels in the mosaic test image (Figure 6), we tested eight different window sizes from 13 by 13 lags to 41 by 41 lags in an increment of four lags (Figure 7 and Figure 8). For each window size, except the window size of 13 that only allowed for one to six lags, eight semi-variance images based on one to eight lags were generated. Classifications were operated based on eight texture bands for each window size. Classification accuracies as measured by the Overall Kappa Coefficient, Conditional Kappa Coefficient, and signature separability of the average Bhattacharrya Distance were computed.

Comparing with Using Gray Value Images and a Building Footprint Image

To verify our hypotheses that a building-presence variogram could represent land-use characteristics better than a pixel-gray-value variogram, we generated semi-variance images based on each of the original gray-value image bands and used for land-use classification (Figure 14). In addition, we conducted land-use classifications based on semi-variance images derived from a building-footprint image that was converted from available building-footprint vector data, since there was confusion between the building class and the pavement class in our initial spectral classification.

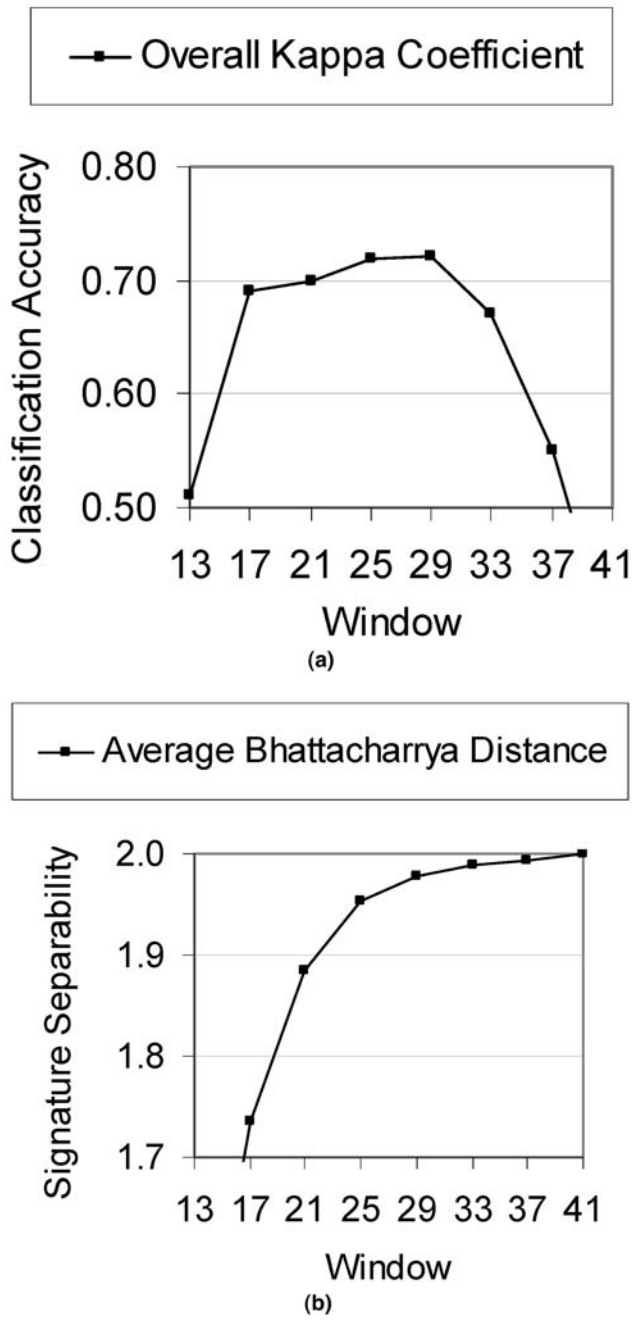

Figure 7. Comparison of (a) classification accuracies, and (b) signature separabilities based on different window sizes. The data point for window 41 is not shown because of its relatively small number.

Results

Single Optimal Window

Comparing classification accuracies based on different window sizes, Figure 7a showed that medium window sizes between 17 to 29 lags achieved higher classification accuracies. The significance test of kappa coefficient from kappa variance further indicated that the difference between window 25 or 29 and others were statistically significant at the 0.99 probability confidence level. The overall trend could be explained that too small or too large

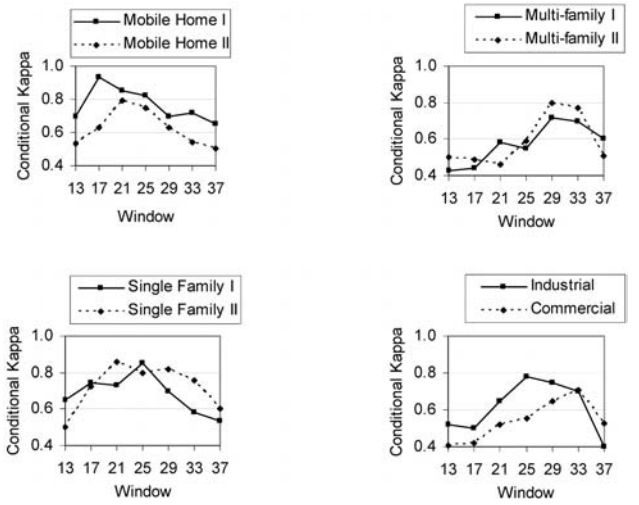

Figure 8. Comparison of conditional Kappa coefficients of land-use classes based on different window sizes.

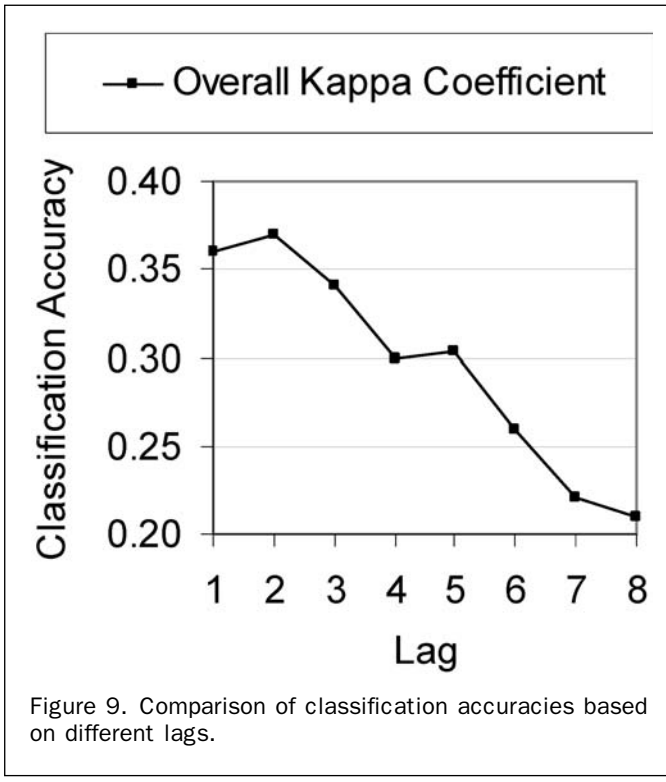

Figure 9. Comparison of classification accuracies based on different lags.

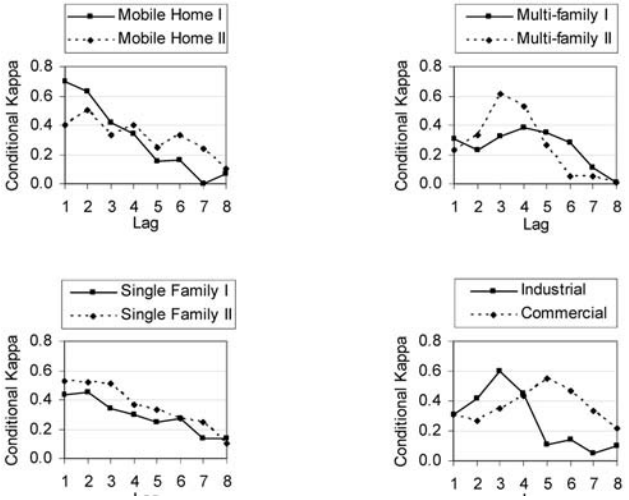

Figure 10. Comparison of conditional Kappa coefficients of land-use classes based on different lags.

window sizes for texture measures did not represent local textures well.

Comparing signature separabilities based on different window sizes, Figure 7b showed that the bigger the window, the higher the signature separability. The overall trend could be explained that the bigger the window size, the more invariant the derived semi-variance signature and the more objective representation of the local texture.

Since optimal windows from classification accuracy did not correspond to those from signature separability, we concluded that signature separability is not a good predictor of classification accuracy in this study. It may be caused by the boundary effect, especially when the window size was large.

Comparing conditional kappa coefficients for land-use classes based on different window sizes, Figure 8 showed that different land-use classes had different optimal window sizes. The optimal window sizes for mobile home I, mobile home II, single family I, single family II, multi-family I, multi-family II, industrial, and commercial were 17, 21, 25, 21, 29, 29, 25, and 33, respectively. Referencing with the mosaic test image in Figure 6, the trend may be explained that for land-use with large buildings or with buildings away from each other, such as multi-family I, multi-family II, and commercial, relatively large window sizes were preferred. On the other hand, for land-use with small buildings or with buildings close to each other, such as mobile home I, mobile home II, and single family II, relatively small window sizes were preferred.

Single Optimal Lag

To investigate the optimal lag, we compared classification accuracies based on different lags. Taking into account the size of window sizes, we tested eight different lags from one lag to eight lags (Figure 9 and Figure 10). For each lag, four semi-variance images based on four optimal window sizes (17, 21, 25, 29) were used for classification. In other words, classifications were operated based on four texture bands for each lag. Figure 9 showed that classification accuracies were generally higher for small lags. The difference of kappa coefficients between lag 1 or lag 2 and others are statistically significant at the 0.99 probability confidence level. There may be two explanations for the overall trend. First, semi-variance of small lags better represented local textures when more data pairs were computed for the semi-variance. Second, semi-variance of small lags were more invariant to the boundary effect since data points for calculating the semi-variance were close together and were more likely to belong to the same class.

Comparing conditional kappa coefficients for land-use classes based on different lags, Figure 10 showed that different land-use classes had different optimal lags. For example, the optimal lags for mobile home I, multi-family II, industrial, and commercial were lag 1, lag 3, lag 3, and lag 5, respectively. Referencing with the mosaic test image in

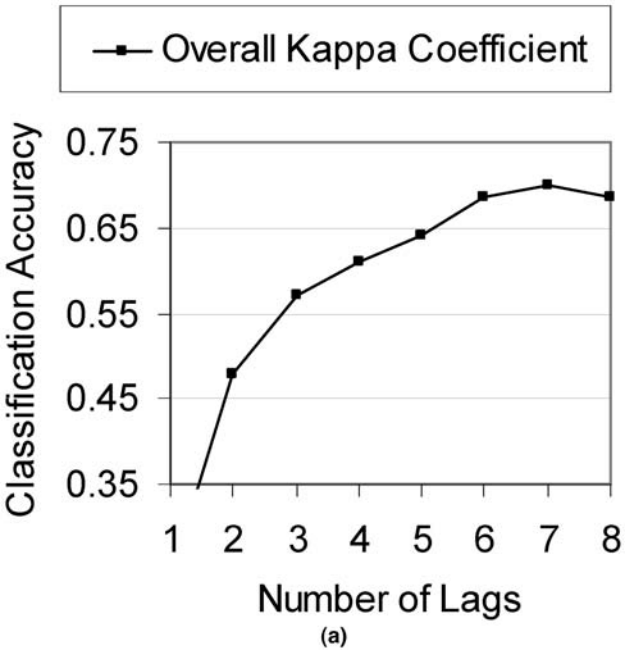

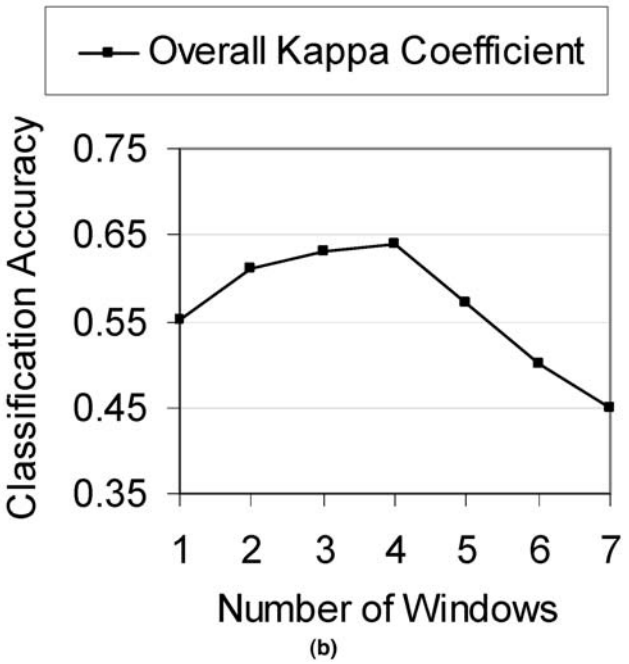

Figure 11. Comparison of classification accuracies based on (a) different numbers of lags, and (b) different numbers of windows.

Figure 6, the trend may be explained that for land-use with small buildings that were close together, such as mobile home I, a relatively short lag distance was preferred. On the other hand, for land-use with large buildings that were far apart, such as commercial, a relatively long lag distance was preferred.

Multiple Optimal Lags and Multiple Optimal Windows

Comparing classification accuracies based on different numbers of lags, compound by their optimality sequence and based on the most optimal window of 29, Figure 11a shows that generally the more number of lags, the higher the classification accuracy. Classification based on seven lags was most accurate and higher than others at the 0.99 probability confidence level. The trend may be explained that the semi-variance for each lag is critical for representing local textures and should be used together for classification.

Comparing classification accuracies based on different numbers of window sizes, compound by their optimality sequence and based on the most optimal lags of one and two, Figure 11b showed that three or four window sizes have the higher classification accuracy than others at the 0.99 probability confidence level. The trend indicated that classifications should not be based on all window sizes. Referencing with the classification accuracies based on individual window sizes (Figure 7a), we concluded that a combination of three or four middle-sized windows (17 to 29) were most accurate.

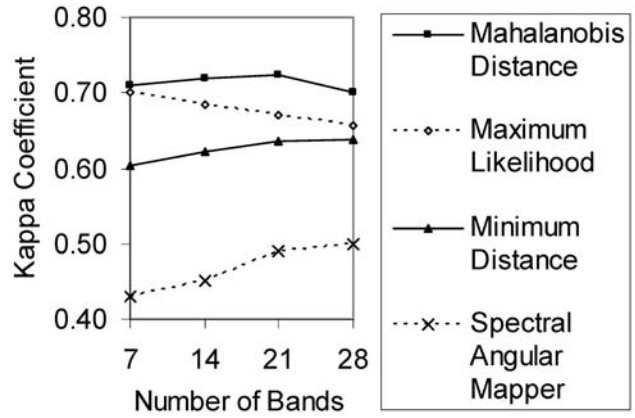

Figure 12. Comparison of classification accuracies based on different numbers of bands and different classifiers.

Optimal Number of Bands and Optimal Classifier

Combining optimal windows and optimal lags, we tested different numbers of texture bands for classification, using different classifiers. Figure 12 showed that classifications using MLC based on 21 or 28 bands were less accurate than that based on 7 or 14 bands, at the 0.99 probability confidence level, while classifications using Minimum Distance Classifier (MM) and Spectral Angular Mapper (SAM) were more accurate when based on more number of bands, in which the difference between 14 and 21 bands was statistically significant. The reason that combining optimal lags and optimal windows did not have compound effects for MLC and Mahalanobis Distance Classification (MDC) may be because the number of training samples did not increase with the number of bands, and thus the estimation of statistical parameters became inaccurate and unreliable (Hughes, 1968; Hsu *et al.*, 2002). MLC and MDC both used probability measures of covariance matrix and were more affected by this Hughes phenomenon, in contrast to MM and SAM that used straightforward Euclidean distance and angular measures.

Figure 12 showed that the most accurate classification was based on three optimal windows, seven optimal lags, with Mahalanobis Distance Classifier (an overall kappa coefficient of 0.72 and an overall classification accuracy of 76 percent). The classification map referenced with ground truth land-use in Figure 13 showed that most of the land-use is correctly classified except the boundary land-use. The confusion matrix in Table 1 showed that mobile home I

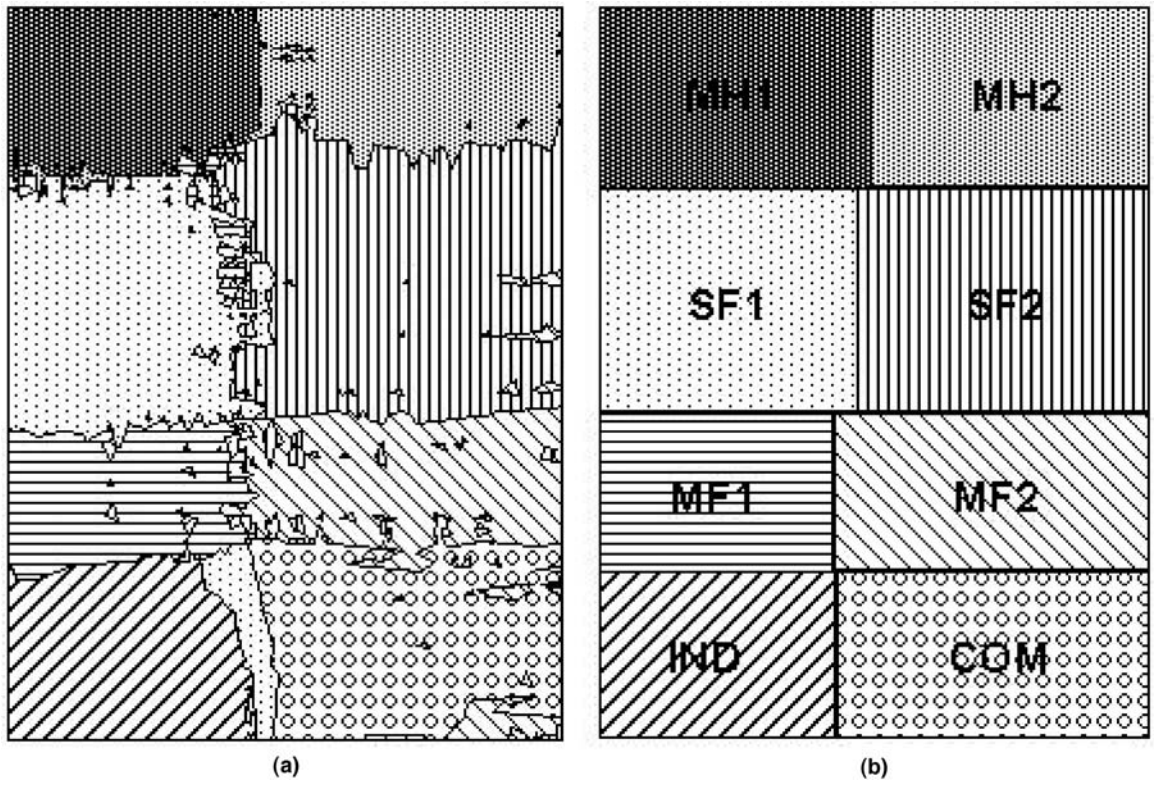

Figure 13. Map of the most accurate classification (a) and ground truth land-use map (b). MH1 is mobile home I; MH2 is mobile home II; SF1 is single family I; SF2 is single family II; MF1 is multi-family I; MF2 is multi-family II; IND is industrial; COM is commercial.

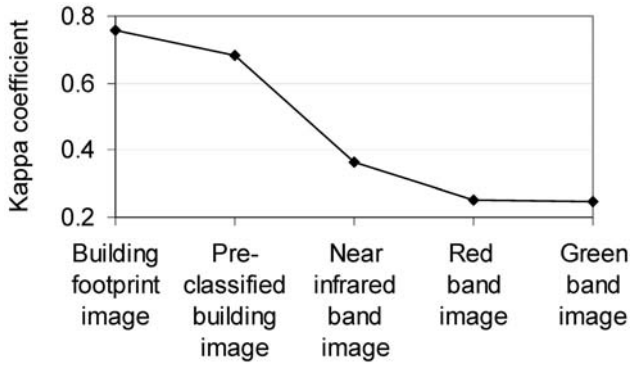

Figure 14. Comparison of classification accuracies based on a building-footprint image, a pre-classified building image, and gray-value band images.

(MH1) and multi-family I (MF1) had the highest omission error of 39 percent and 69 percent mainly from misclassifying into their neighboring land-use of mobile home II (MH2) and multi-family II (MF2) respectively.

Comparison with Using Gray Value Images and a Building Footprint Image

Figure 14 showed the comparison of texture analysis based on a building-footprint image, a pre-classified building-presence image, and three gray-value image bands. Classifications were all based on 14 optimal texture bands using MLC. The results supported our hypothesis that a variogram-based texture analysis was more accurate when based on building-presence image than pixel-gray-value image, especially when the building-presence image was derived from existing building footprint inventory data.

Discussion

The main constraint of applying a building-presence variogram for urban land-use classification is that land-uses without buildings, with few buildings, or with buildings that do not have homogeneous spatial patterns or do not relate to land-use types would be hard to classify. Particularly the contemporary trend of the architectural design of buildings seems to promote uniqueness and diversity. Varied styles of neighborhoods with different spatial patterns of buildings are being constructed nowadays, which makes it difficult to establish standard spatial patterns for land-use classes. Also, variogram analysis modeled in an area at a time may not be applicable to another area at another time when the spatial patterns of buildings are so varied.

Future research could test the variogram analysis based on a classified land-cover map, in contrast to a classified building map, for inferring urban land-use. In this approach, pixels of each land-cover class could be assigned a mean spectral value of the class before calculating the variogram. The rationale is to test whether or not spatial patterns between land-cover classes relate to land-use classes. In a similar way, the variogram analysis could be based on a spectral cluster map from unsupervised classification or gray-level reduction algorithms. Another possible approach is to use a cross-variogram (Chica-Olmo and

TABLE 1. CONFUSION MATRIX FROM ACCURACY ASSESSMENT (MH1 IS MOBILE HOME I; MH2 IS MOBILE HOME II; SF1 IS SINGLE FAMILY I; SF2 IS SINGLE FAMILY II; MF1 IS MULTI-FAMILY I; MF2 IS MULTI-FAMILY II; IND IS INDUSTRIAL; COM IS COMMERCIAL)

Reference Data \ Classified Data	MH1	MH2	SF1	SF2	MF1	MF2	IND	COM	Total	Commission Error
MH1	27								27	0%
MH2	14	44	3	5					66	33%
SF1	2	1	54	12	16		9	4	98	45%
SF2				66		1			67	1%
MF1					15				15	0%
MF2			1	3	18	33		6	61	46%
IND							22		22	0%
COM	1							43	44	2%
Total	44	45	58	86	49	34	31	53	400	
Omission Error	39%	2%	7%	23%	69%	3%	29%	19%		76%

Abarca-Hernández, 2000) to measure the spatial relationship between two land-cover classes, such as the building class and the vegetation class, for inferring urban land-use.

Summary and Conclusions

This study tested the effectiveness of a variogram-based texture analysis in the classification of urban land-use using a mosaic test image of eight land-use classes. Optimal window sizes, lags, numbers of texture bands, and classifiers were also investigated. The best classification result was considered satisfactory with 0.72 overall Kappa coefficient and 76 percent overall accuracy.

Some of the major findings from the analysis include:

- Different classes showed different optimal lags and optimal window sizes. Generally larger window sizes and longer lags were preferred for land-use with large buildings or buildings that were far apart, while smaller window sizes and shorter lags were preferred for land-use with small buildings or buildings that were close to each other.
- Texture bands based on all different lags could capture the full spectrum of spatial characteristics and achieved higher classification accuracy.
- Texture bands based on a few middle window sizes, specifically windows 17, 21, 25, and 29, could avoid the boundary effect and achieved higher classification accuracy.
- Variogram analysis based on a building-footprint image was more accurate than based on a pre-classified building image, while the analysis based on a pre-classified building image was more accurate than based on a gray-value image.

Land-use classification for the urban areas gets more difficult when urban land-use parcels are small and segmented. It is common today that city planners do not plot large, homogeneous land-use parcels as before, since the sustainable trend in land-use planning is to promote mixed land-use and encourage urban density instead of continuing the homogeneous and sprawled land-use tradition. Variogram-based texture analysis with high spatial resolution remote sensing images may provide a way to classify urban land-use. Future research needs to test how accurate variogram-based texture analysis can classify small parcels of a variety of detailed land-use types.

References

Berberoglu, S., C.D. Lloyd, P.M. Atkinson, and P.J. Curran, 2000. The integration of spectral and texture information using neural networks for land cover mapping in the Mediterranean, *Computers and Geosciences*, 26(4):385–396.

Burrough, P.A., and R. McDonnell, 1998. *Principles of Geographical Information Systems*, Oxford University Press, New York, 333 p.

Carr, J.R., 1996. Spectral and texture classification of single and multiple band digital images, *Computers and Geosciences*, 22(8):849–865.

Chen, D.M., and D. Stow 2002. The effect of training strategies on supervised classification at different spatial resolutions, *Photogrammetric Engineering & Remote Sensing*, 68(11): 1155–1161.

Chen, Q., and P. Gong, 2004. Automatic variogram parameter extraction for texture classification of the panchromatic IKONOS imagery, *IEEE Transactions on Geoscience and Remote Sensing*, 42(5):1106–1115.

Chica-Olmo, M., and F. Abarca-Hernández, 2000. Computing geostatistical image texture for remotely sensed data classification, *Computers and Geosciences*, 26(4):373–383.

COA (City of Austin), 2001. *Austin Area Population Histories and Forecasts*, City of Austin, URL: http://www.ci.austin.tx.us/census/downloads/austin_forecast01.xls (last date accessed: 24 April 2006).

Donnay, J.P., M.J. Barnsley, and P.A. Longley, 2001. Remote sensing and urban analysis, *Remote Sensing and Urban Analysis* (J.P. Donnay, M.J. Barnsley, and P.A. Longley, editors), Taylor & Francis, London and New York, 268 p.

Gong P., and P.J. Howarth, 1992. Frequency-based contextual classification and gray-level vector reduction for land use identification, *Photogrammetric Engineering & Remote Sensing*, 58(4):423–437.

Gong, P. 1994. Reducing boundary effects in a kernel-based classifier, *International Journal of Remote Sensing*, 15(5): 1131–1139.

Herzfeld, U.C., and C.A. Higginson, 1996. Automated geostatistical seafloor classification- principles, parameters, feature vectors and discrimination criteria, *Computers and Geosciences*, 22(1):35–41.

Hsu, P., Y. Tseng, and P. Gong, 2002. Dimension reduction of hyperspectral images for classification applications, *Geographic Information Sciences*, 8(1):1–8.

Hughes, G.F., 1968. On mean accuracy of statistical pattern recognizers, *IEEE Transactions on Information Theory*, 14(1): 55–63.

Lark, R.M., 1996. Geostatistical description of texture on an aerial photograph for discriminating classes of land cover, *International Journal of Remote Sensing*, 17(11):2115–2133.

Maillard, P., 2003. Comparing texture analysis methods through classification, *Photogrammetric Engineering & Remote Sensing*, 69(4):357–367.

Miranda, F.P., and J.R. Carr, 1994. Application of the semivariogram texture classifier (STC) for vegetation discrimination using SIR-B data of the Guiana Shield, Northwestern Brazil, *Remote Sensing Reviews*, 10:155–168.

Miranda, F.P., J.A. Macdonald, and J.R. Carr, 1992. Application of the semivariogram texture classifier (STC) for vegetation discrimination using SIR-B data of Borneo, *International Journal of Remote Sensing*, 13(12):2349–2354.

Ramstein, G., and M. Raffy, 1989. Analysis of the structure of radiometric remotely-sensed images, *International Journal of Remote Sensing*, 10:1049–1073.

Xu, B., P. Gong, R. Spear, and E. Seto, 2003. Comparison of different gray level reduction schemes for a revised texture spectrum method for land use classification using Ikonos imagery, *Photogrammetric Engineering & Remote Sensing*, 69(5):529–536.

(Received 24 March 2005; accepted 10 May 2005; revised 07 June 2005)